Numerical Study of Natural Convection in Square Tilted Solar Cavity Considering Extended Domain

Arrif, T., Chehhat, A., Abo-Serie, E. & Benchabane , A.

Numerical Study of Natural Convection in Square Tilted Solar Cavity Considering Extended Domain

Toufik Arrif[1, 2], Abdelmadjid Chehhat[3, 4, *], Essam Abo-Serie[5] and Adel Benchabane[2]

Abstract: This work presents a numerical investigation on heat transfer and fluid-dynamic aspects for a solar open cavities in an extended fluid flow domain. The vertical wall inside the open cavities facing the aperture is assumed to be isothermal while the other walls are kept insulated. Heat transfer steady laminar natural convection is studied by solving the non-dimensional governing equations of mass, momentum and energy in the framework of a finite volume method. The analysis are carried out under Rayleigh number range of 9.41×10^5 to 3.76×10^6, inclination 0° to 90° and opening ratio 0.25, 0.5 and 1. The model results for avaergar Nusselt number evaluation was in good agreement with other published work for similar configuration. The results show that convective average Nusselt number decreases by 93% when the inclination angle increased from 0° to 90° due to the trapped vortices that limit the airflow throughout the cavity. The air flowing through the cavit is maximum when the the inclination angle is zero even at higher values of Raylight number. Results show also that decreasing the opening ratio from 1 to 0.25 leads to a drop in heat loss by 22.79%. A simple correlation has been developed for calculating the the average Nusselt number as a function of Rayleigh number, opening ratio and inclination angle.

Keywords: Natural convection, finite-volume method, average Nusselt number, solar cavity, Rayleigh number.

Nomenclature

A   Wall surface, (m^2)

a/H Opening ratio (Aperture Height)/(Cavity Height)

a   Aperture Height, (m)

g   Acceleration due to gravity, (m/s^2)

[1] Unité de Recherche Appliquée en Energies Renouvelables, URAER, Centre de Développement des Energies Renouvelables, CDER, 47133, Ghardaïa, Algérie.

[2] Université Mohamed Khider Biskra, Département de génie mécanique, Laboratoire de Génie énergétique et matériaux « LGEM », BP 145, RP07000, Biskra, Algérie.

[3] Université Abbes Laghrour Khenchela, Faculté des Sciences et de la Technologie, Département de génie mécanique, 40000, Khenchela, Algérie.

[4] Laboratoire des études des systèmes énergétiques industriels « LESEI », Université de Batna 2 , Algérie.

[5] Coventry University, School of Mechanical, Aerospace and Automotive Engineering, Coventry, UK.

* Corresponding Author: Abdelmadjid Chehhat. Email: achehhat@gmail.com.

h   Average convective coefficient, $(W/m^2.K)$

H   Cavity height, (m)

k   Thermal conductivity, (W/m.K)

L   Cavity width, (m)

Nu_c Average convective Nusselt number, (hL/k)

P   Dimensionless pressure, $(p-p_\infty)H^2/\rho\alpha^2$

p   Pressure, (Pa)

Pr   Prandtl number, (ν/α)

Q_C Convective heat loss, (W)

Ra   Rayleigh number, $(g\beta\Delta TH^3/\nu\alpha)$

S_P Source term in the generalized differential equation

T   Temperature, (K)

u   Velocity component in x-direction

U   Dimensionless fluid velocity, u/U_0 in x-direction

U_0 Reference velocity, $(g\beta H(T-T_a))^{(1/2)}$

v   Velocity component in y-direction

V   Dimensionless fluid velocity, v/U_0 in y-direction

x,y   Cartesian coordinates

X,Y   Dimensionless Cartesian coordinates, x/H, y/H

Greek symbols

α Thermal diffusivity, (m^2/s)

β Volumetric coefficient of thermal expansion, (K^{-1})

$\Delta x, \Delta y$ Grid spacing of volume control, (m)

θ Dimensionless temperature, $(T-T_\infty)/(T_H-T_\infty)$

ν Kinematic viscosity, m^2/s

ρ Fluid density, kg/m^3

Φ Independent variable in the generalized differential equation.

φ Inclination angle of the cavity from the vertical (°).

Ψ Stream function

ω Dimensionless temperature difference $(\Delta T)/T_\infty$

Subscripts

∞ Ambient

H   Hot wall

Max   Maximum

1 Introduction

Renewable energy is considered as clean, with no pollutants. Solar thermal energy system has received a great attention around the world. This system uses concentrator to produce electricity by employing a parabolic trough, mirror (linear Fresnel collectors, LFC) system, dish/Stirling and a concentrated solar power tower. The concentrated solar power tower called CRS (Concentrated Receiver System) contains several mirrors called "heliostats" (Greek: Which fixes the sun) which are positioned around the tower. These heliostats reflect solar rays into a cavity (absorber) which rises fluid (air, water, molten salts, etc.) temperature to more than 1000°C [Zhang, Baeyens and Degreve (2013)].

In solar cavity receiver, the radiation reflected by the heliostats passes through an aperture and reach the inner wall of the receiver.

A solar cavity receiver has been proposed and developed in order to achieve high operating temperature level. Nevertheles, the rate of heat loss need to be reduced particularly the convective heat transfer in windy conditions. In fact, evaluating the heat losses is not easy, due to the interaction of several parameters and the receiver complex geometries. In addition to the existence of the three mechanism of heat transfer; conduction, convection and radiation. Conduction heat loss occurs through the insulated walls while convective and radiative heat losses occure through the aperture [Ka lok, Jafarian and Farzin (2017)]. The convective heat losses occurs as a result of both free convection that is driven by buoyancy, and forced convection, that is driven by any wind current. Having comples spatial and temporal variation in the flow field makes evaluating the heat flux and loss not an easy task and thereofor assumptions inside and around the cavity have to be applied. On the other hand, heat losses by conduction and radiation can be predicted analytically using absorptivity, emissivity. This paper is focused on performing numerical study to study the effect of the geometrical and thermal parameters on the convective heat loss from open solar cavities.

A large number of numerical studies have been carried out to describe the natural convection in a solar cavity receiver in the literature. Clausing [Clausing (1981)] presented an analytical model which estimates the convective heat loss from the receive cavity and observed that the buoyancy induced in the cavity is a major factor in transferring energy across the aperture. Chan et al. [Chan and Tien (1985)] investigated numerically the laminar steady state natural convection in two-dimensional rectangular open cavity. They found that the flow patterns and heat transfer are governed by the characteristics of the heated cavity. Their analysis are found to be in good agreement with the experimental data for: Ra=10^6. Angirasa et al. [Angirasa, Pourquié and Nieuwstadt (1992)] studied the transient and steady laminar natural convection in a square open cavity. They used the vorticity- stream function formulation and concluded that the natural convection does not depend on the computational domain or the boundary conditions on the open side of the cavity. Angirasa et al. [Angirasa, Eggels and Nieuwstadt (1995)] presented a numerical simulation for buoyancy-induced flow and heat transfer in a square isothermal open cavity and evelauted the Nusselt number for steady and unsteady flows. They observed also periodic and unsteady flows at moderate and high Rayleigh number. Mohamad [Mohamad (1995)] presented a flow pattern and heat transfer as a result of the natural convection in open cavities with a heated plates

attached with a parallel vertical strips at Rayleigh number 10^3 to 10^7, inclination 10° to 90°. They found that the average Nusselt number is insensitive to the cavities inclination. Chakroun et al. [Chakroun, Elsayed and Al-Fahed (1997)] investigated experimentally the heat transfer coefficient from a rectangular tilted cavity, considering a constant heat flux as a boundary condition at the wall opposing the aperture. They concluded that the parameters: Grashof number, tilt angle, aspect ratio (height-to-width of the cavity) and opening ratio (opening height to cavity height) affect the average heat transfer coefficient between the cavity and the ambient air. Hinojosa et al. [Hinojosa, Cabanillas and Alvarez (2005)] presented a numerical simulation of the heat transfer by natural convection and surface thermal radiation in a tilted open cavity. The results indicated that Nusselt number increases with Rayleigh number except at a tilted angle of 180°, but the radiative Nusselt number is insensitive to the orientation of the cavity. Humphrey et al. [Humphrey and Sherman (1985)] studied and investigated experimentally the effects of cavity shape, inclination and ambient wind, on the velocity and temperature distribution inside a rectangular open cavity for both free and forced convection. For free convection, they found that the rate of convective heat loss across the cavity aperture plane is reduced by both the increase in aspect ratio and inclination angles. Elsayed et al. [Elsayed, Al-Najem and El-Refaee (1999)] presented a numerical simulation of two-dimensional laminar natural convection in a fully open cavity with a back wall at constant temperature. The effect of tilt angle (-60° to 90°) and Grashof number (10^2 to 10^5) on the heat transfer. They concluded that the Nusselt number of the open cavity is similar to that of a flat plate if the Grashof number and tilt angle are increased. Penot [Penot (1982)] investigated a natural convection inside an isothermal open square cavity. They analyzed the effect of Grashof number and inclination of the cavity and their results showed that the unsteady movement in the cavity is due to two factors; the first is thermal and occur when $Gr>10^5$ for a vertical cavity, the second is of hydrodynamic origin and it occur when the cavity faces upward. Miyamoto et al. [Miyamoto, Kuehn and Goldstein (1989)] studied numerically the laminar natural convection heat transfer in a two-dimensional partially or fully open square cavity with three walls heated at a uniform temperature. They concluded that the dimensionless flow rate through the cavity with all walls heated is about twice the flow rate through the cavity with a heated back wall and two insulated walls. Wang et al. [Wang, Yang and Li (2011)] reported a numerical simulation of the combined convection-conduction and surface radiation in an open cavity heated by constant flux. Results showed that emissivity and conductivity ratio increase the average total Nusselt number. They conclude that the increase due to radiation extends from 54.1% to 64%. Adnani et al. [Adnani, Meziani and Ourrad (2016)] presented a numerical study of natural convection in a square cavity with sidewalls exposed to thermals boundary conditions. The effect of Prandtl and Rayleigh numbers, flow field, stream functions, horizontal velocity, local and average Nusselt numbers on the flow field were discussed. Their results showed that for very high Rayleigh numbers the heat transfer decreases with increasing Prandtl number. However, at low Rayleigh numbers the flow field is slightly pronounced with increasing Prandtl number. Bensouici et al. [Bensouici and Boudebous (2017)] performed a numerical investigation of the laminar forced convection in lid driven square enclosure with a central square and isotherm heat source. They used a Water Nano fluid to analyze the heat transfer with four types of naco pacticles: Cu, Ag,

Al_2O_3 and TiO_2. They studied the impact of Richardson number, the size of the heat source, solid volume fraction and type of nanofluid on the heat transfer characteristics of the forced convection. Their major finding was that, the combination of three parameters which are: Size S=0.25 for copper-water nanofluid at Ri=100 will better cool the heat source. Manoj et al. [Manoj and Rajsekhar (2018)] reported a numerical investigation to examine the free convection of a right-angled triangular cavity filled with water for four different configurations. The effect of sinusoidal hot wall, partially active cold walls' configurations and Rayleigh number (10^5-10^7) on fluid flow and heat transfer were examined. The results revealed that if the two parameters: The sinusoidal hot wall and the cold walls, configuration AB, are merged the heat transfer will be pronounced. Heat and mass transfer behavior occuring in a cavity filled with a low Prandtl number liquid has been studied by Nouri et al. [Nouri, Ghezal and Abboudi (2018)]. The influence of the parameters such as, Lewis and Prandtl numbers, on the instability of the flow was also studied. The results showed the dependence of unicellular and multicellular flows formation on the Prandtl number.

Considering the above literature, the aim of this numerical study is to analyze the heat transfer for a laminar natural convection condition inside solar open cavities. Heat transfer and flow are evaluated under the following geometrical and thermal parameters: opening ratio a/H, inclination φ, and Rayleigh number Ra. It is seen from the literature review that solar open cavity has not been studied with the following cases: temperature imposed on the side wall (vertical wall), cavity inclination (0°, 15°, 30°, 45°, 60°, 75°, 90°), opening ratio a/H (0.25, 0.5 and 1), Rayleigh number Ra (9.41×10^5 to 3.76×10^6). However all the studies were limited to the cavity. In this study the domain has been extended beyond the cavity.

2 Physical model and governing equations

The heat transfer in a two-dimensional square tilted open cavity of length L, height H and opening ratio a/H is considered in the present investigation as shown in Fig. 1.

The cavity is inclined at angle φ with respect to vertical. The opposite wall to the aperture was kept at a constant temperature T_H while the surrounding fluid interacting with the aperture was fixed to an ambient temperature T_∞. The remaining internal and external cavity walls were insulated. The assumptions considered in this work are: The fluid is air (Pr=0.71), Newtonian, fluid flow is laminar, viscous dissipation and work of compression are negligible. The fluid properties are assumed constant except for the density in the buoyant force term in the momentum equations (Boussinesq approximation), radiation heat transfer and conduction in the solid region are negligible. The governing equations of continuity (Mass), momentum, and energy formulated in 2-D Cartesian coordinates take the dimensionless form:

$$\frac{\partial U}{\partial X} + \frac{\partial V}{\partial Y} = 0 \tag{1}$$

$$U\frac{\partial U}{\partial X} + V\frac{\partial U}{\partial Y} = -\frac{\partial p}{\partial X} + \left(\frac{Pr}{Ra}\right)^{\frac{1}{2}} + \left(\frac{\partial^2 U}{\partial X^2} + \frac{\partial^2 U}{\partial Y^2}\right) + \theta\sin\varphi \tag{2}$$

$$U\frac{\partial V}{\partial X} + V\frac{\partial V}{\partial Y} = -\frac{\partial p}{\partial Y} + \left(\frac{Pr}{Ra}\right)^{\frac{1}{2}} + \left(\frac{\partial^2 V}{\partial X^2} + \frac{\partial^2 V}{\partial Y^2}\right) + \theta\cos\varphi \qquad (3)$$

$$U\frac{\partial \theta}{\partial X} + V\frac{\partial \theta}{\partial Y} = \frac{1}{(PrRa)^{1/2}} + \left(\frac{\partial^2 \theta}{\partial X^2} + \frac{\partial^2 \theta}{\partial Y^2}\right) \qquad (4)$$
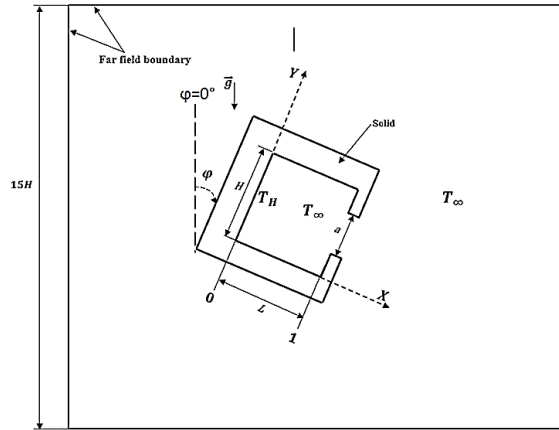

Figure 1: Physical domain and configuration geometry of cavity

Eq. (1) represents the overall mass balance in a differential volume at a fixed location. Eqs. (2) And (3) represent the momentum equation for Newtonian fluids in X and Y directions. Eq. (4) is the energy equation applied to a differential volume of fluid.

$Ra = g\beta\Delta TH^3/(\nu\alpha)$ is the Rayleigh number, and $Pr = \nu/\alpha$ is the Prandtl number. The above dimensional equations were obtained by defining the following dimensionless parameters:

$$X = x/H, Y = y/H, P = \frac{(p - p_\infty)H^2}{\rho\alpha^2}, U = u/U_0, V = v/U_0,$$

$$\theta = (T - T_\infty)/(T_H - T_\infty)$$

The reference velocity U_0 is related to the buoyancy force term and was defined as:

$$U_0 = (g\beta H(T - T_\infty))^{1/2}$$

The Eqs. (1)-(4) are solved in the steady-state form. The computational grid and boundary conditions of the cavity receiver is expressed in Fig. 2(a) and an enlarge view of mesh is shown in Fig. 2(b), where label mark represents (1) Cavity Receiver, (2) Extended Domain, and (3) Pressure Inlet. This open square cavity is surrounded by an extended domain. The domain was increased until it was having a minimum effect on fluid and heat flows adjacent to the open cavity. To achieve this, it was found that the size of the square enclosure should be about fifteen times the height of the open cavity. In this work we used structured grid that insures convergence and efficiency. The location of the nodes inside the cavity is selected with stretching function so that the node density in X and Y direction is higher near the walls of the cavity Fig. 2(b). Fig. 3 shows the representation of solar power tower plant system and the placement of the solar cavity

receiver. If velocities are defined at scalar nodes then the influence of pressure is not properly represented in the discretized momentum equations, a remedy for this problem a staggered grid for velocities is employed**.** Therefore, the scalar variable such as pressure and temperature are stored at the nodes marked (●) (P, E, W, N, S), but the velocities are stored at the scalar cell faces (e, w, n, s) and are indicated by arrows], as shown in Fig. 4 [Versteeg and Malalasekera (1995)].
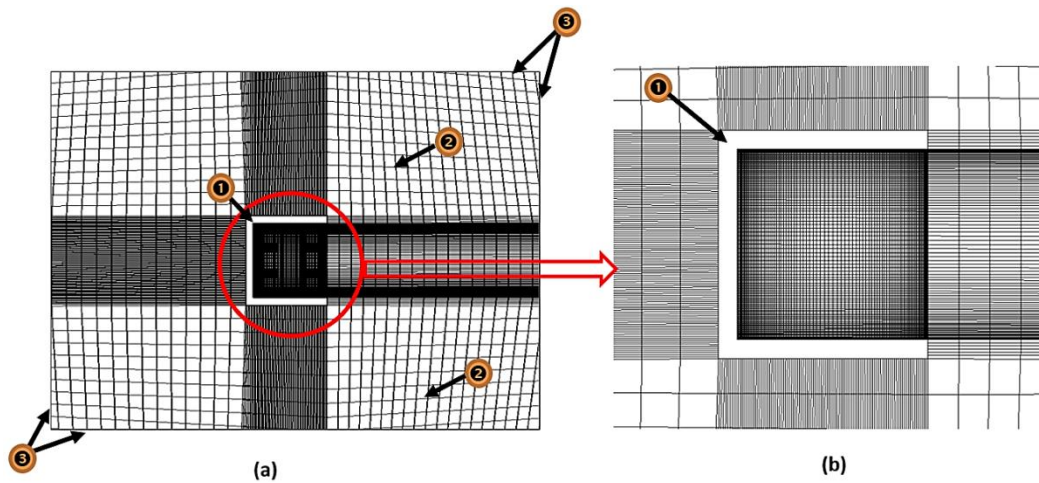

(a)   (b)

Figure 2: (a) Computational grid of the cavity receiver: (89860) nodes in the extended domain. (b) Enlarge view of a mesh (130×130)

Labels: ❶Cavity Receiver, ❷Extended Domain, ❸ Pressure Inlet
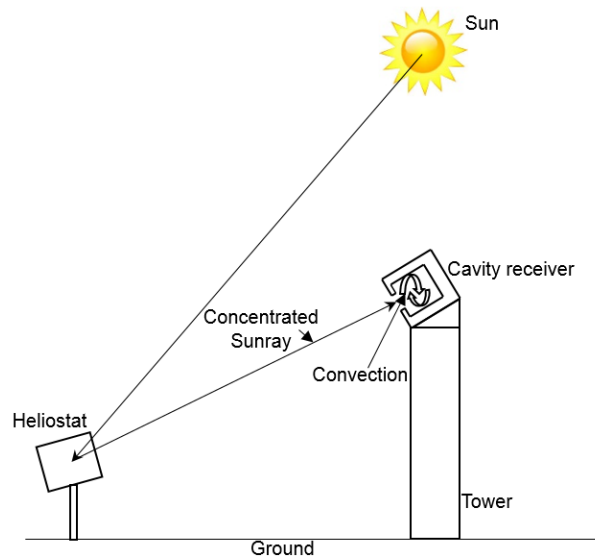

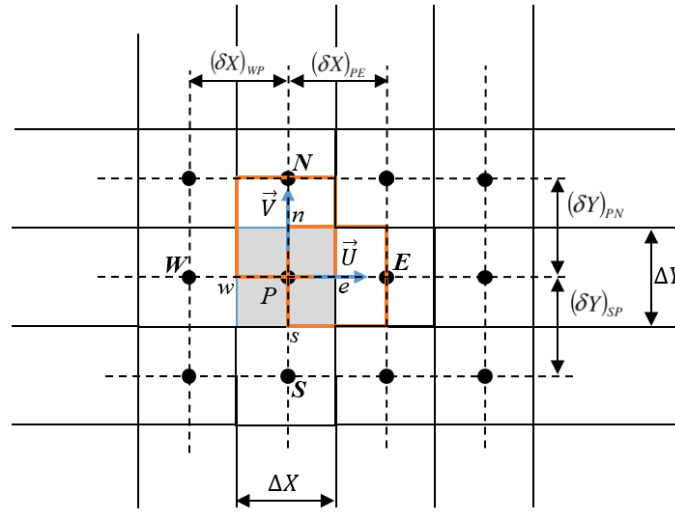**Figure 3:** Schematic representation of solar power tower plant

Figure 4: The arrangement of the control volume for a two dimensional flow with staggered grid definition

2.1 Boundary conditions

Versteeg et al. [Versteeg and Malalasekera (1995)] state that, for the far field boundary conditions, the characteristics of the flow inside and immediately in front of a cavity do not differ significantly from those calculated by simply specifying zero normal gradients for all variables everywhere along the far field boundaries. At the far field boundaries, temperatures of fluid coming from the ambient region are set to zero while the temperatures of the fluid exiting satisfies the upwind condition, assuming convection to be predominant. The boundary condition for U, the horizontal velocity and V, the vertical velocity are obtained by the mass balance at the boundary cells. The mathematical representations of the boundary conditions are listed below:

Far field boundary:

$$\frac{\partial U}{\partial X} = -\frac{\partial V}{\partial Y}(0 < Y < 15H) \tag{5}$$

$$\frac{\partial V}{\partial Y} = -\frac{\partial U}{\partial X}(0 < X < 15H) \tag{6}$$

$$\frac{\partial \theta}{\partial X} = 0 \;\; \text{if } U > 0 \text{ and } \;\; \theta = 0 \;\; \text{if } U < 0 \qquad (0 < Y < 15H) \tag{7}$$

$$\frac{\partial \theta}{\partial Y} = 0 \;\; \text{if } V > 0 \text{ and } \;\; \theta = 0 \;\; \text{if } V < 0 \qquad (0 < X < 15H) \tag{8}$$

$$P(X, Y) = 0 \quad , \quad (0 < Y < 15H) \;\; \text{and} \;\; (0 < X < 15H) \tag{9}$$

Vertical hot wall:

$$\{U \;\; \text{and} \;\; (0 < X < 15H) \tag{10}$$

$$\begin{cases} U = V = P = 0 & (0 < Y < H) \\ \theta = 1 & (0 < Y < H) \end{cases} \tag{11}$$

Internal and external cavity walls:

$$\begin{cases} U = V = 0 \\ \dfrac{\partial \theta}{\partial X} = 0 \\ \qquad \dfrac{\partial \theta}{\partial Y} = 0 \end{cases} \tag{12}$$

The average Nusselt number is calculated as:

$$\overline{Nu_c} = \int_0^1 \left(-\frac{\partial \theta}{\partial X} \right) dY \tag{13}$$

Where the subscripts 0 and 1 in Eq. (13) are at: $Y = 0$ and H respectively.

The average heat transfer coefficient (convective coefficient) is calculated as:

$$h = \frac{\overline{Nu_c} \times k}{L} \tag{14}$$

The heat transfer loss (convective heat loss) is calculated as:

$$Q_c = h \times A \times \Delta T \tag{15}$$

The stream function Ψ is calculated from its definition as:

$$U = -\frac{\partial \Psi}{\partial Y} \tag{16}$$

$$V = \frac{\partial \Psi}{\partial X} \tag{17}$$

3 Numerical approach

The finite volume method is used for the discretization of conservation laws; continuity, momentum and energy. The problem of the coefficients discontinuities involved in the equations has be resolved by choosing the mesh such that the discontinuities of the coefficients occur at the boundaries of the control volumes [Le Quere, Humphrey and Sherman (1981)]. The conservation equations can be written in a common format to avoid repeating the work of discretization for each equation. If we denote the variable ϕ in each of the equations: Conservation equations can be reduced to one general equation in Cartesian coordinates in the form:

$$\frac{\partial}{\partial x}(U\phi) + \frac{\partial}{\partial y}(v\phi) = \frac{\partial}{\partial x}\left(\Gamma \frac{\partial \phi}{\partial x} \right) + \frac{\partial}{\partial y}\left(\Gamma \frac{\partial \phi}{\partial y} \right) + \overline{S_\emptyset} \tag{18}$$

The various terms of the generalized equation are listed in Tab. 1.

The SIMPLER algorithm (Semi-Implicit Method for Pressure Linked Equations Revised) scheme is used to couple the continuity and momentum equations [Eymard, Gallou and Herbin (2000); Patankar (1980)]. The governing equations are converted into a system of algebraic equations by means of integration over each control volume of the domain. The Tridiagonal Matrix Inversion Algorithm (TDMA) was then used to sweep the domain of integration along the two axes. The the second order upwind scheme is used in when discretizing momentum and energy equations. The convergence criteria, for mass and momentum are set when their residuals are less than 10^{-4}, while for the energy equation is

10^{-6}. Once the convergence criteria are satisfied, the iteration stops and the solution is obtained.

Table 1: Equivalence terms between generalized equation and dimensionless equations

Conservation equations	ϕ	Γ	S_ϕ
Mass (1)	1	0	0
Momentum in x (2)	U	$\left(\dfrac{Pr}{Ra}\right)^{\frac{1}{2}}$	$-\dfrac{\partial p}{\partial X} + \theta\sin\varphi$
Momentum in y (3)	V	$\left(\dfrac{Pr}{Ra}\right)^{\frac{1}{2}}$	$-\dfrac{\partial p}{\partial Y} + \theta\cos\varphi$
Energy (4)	θ	$(PrRa)^{-1/2}$	0

4 Mesh independence and code validation

The mesh independence study was conducted for Rayleigh number of 3.76×10^6 and inclination angle $\varphi=0°$. The corresponding average Nusselt number Nu_c and convective heat loss Q_c (Watt) values are then evaluated for various cell numbers as listed in Tab. 2. The mesh independence was carried out by examining the value of average Nusselt number. When the difference in the computed values of average Nusselt number between two consecutive mesh sizes is less than 0.5% the mesh was considered independent and all the subsequent cases are carried out for this specific mesh size. Based on that a non-uniform grid of 130×130 inside the cavity (16900 nodes, and 89860) nodes in all domains is selected. The computer code which is based on the formulation presented above was validated against the results reported by previous publications [Mohamed (1995); Chakroun, Elsayed and Al-Fahed (1997); Hinojosa, Cabanillas and Alvarez (2005)].

Table 2: Grid independency based on the values of average Nusselt numbers $\overline{Nu_C}$ and Q_C

Elements in Mesh	Q_C (W)	Change (%)	Nu_C	Change (%)
80 × 80	2.33	--	22.03	--
100 × 100	2.18	6.40	20.66	6.20
120 × 120	2.16	0.88	20.51	0.73
130 × 130	2.15	0.23	20.47	0.20
140 × 140	2.15	0.09	20.46	0.06

The average Nusselt numbers Nu_c is calculated on the hot wall for different Rayleigh numbers and the results are compared with three previous publications as listed in Tab. 3. As shown in the table three a good agreement between the results obtained by the current model and other published data.

Table 3: Comparative analysis of average Nusselt numbers $\overline{Nu_C}$ on the hot wall for different Rayleigh numbers Ra

	Present Work (extended domain)	[Hinojosa, Cabanillas and Alvarez (2005)]	[Mohamed (1995)]	[Chakroun, Elsayed and Al-Fahed (1997)]
Ra				
1×10^4	3.41	3.44	3.44	-
1×10^5	7.44	7.44	7.41	-
1×10^6	14.50	14.51	14.36	-
6.3×10^6	23.89	-	-	24
1×10^7	27.13	27.58	28.6±2.5	-

5 Results and discussion

In order to understand the effect of inclination φ, Rayleigh number Ra and opening ratio a/H on the heat transfer phenomena, stream lines and temperature field in the square cavity are plotted and examined. In the following sections, the flow stream lines and temperature contour for opening ratio 0.5 and φ=0° for different value of Rayleigh number , opening ratio and inclination will be presented first and then their effect on the average convective Nusselt number and heat loss will be presented and discussed.

5.1 Temperature and flow field

Streamlines and temperature are presented in Figs. 5 (a-b-c-d) for Rayleigh number from $9.41×10^5$ to $3.76×10^6$. It can be observed that the convective heat transfer dominates and flow streamlines covers the entire internal space of the cavity.

As shown from Fig. 5, the cold air enters through the lower side of the opening, pushing the air from the bottom of the cavity upwards along the vertical hot wall and discharging it to the outside from the upper side of the opening. As Rayleigh number increases the cold air admitted into the cavity also increases with a tendency of creating a larger vortex at the bottom side of the cavity. The vortex is attributed to the sudden flow expansion inside the cavity. The increase in the size of the circulation zone may be attributed to the increase in the buoyancy force that causes low pressure zone at the bottom leading to acceleration of the cold air towards the bottom of the hot wall. The isotherms show the formation of thinner layer in the vertical hot wall with higher velocity with increasing Rayleigh number. This is explained by the creation of a colder region in the lower region of the cavity.

Fig. 6 shows the effect of opening ratio for : a/H = 1 (larger opening) and a/H = 0.25 (smaller opening). The case for a/H = 0.5 is shown in Fig. 5(d). For both streamlines and temperature, we can see that convection is enhanced for a/H = 1 But the cold fluid acceleration is higher for a/H = 0.25. It is noticeable that at a/H =0.25 the air entering the cavity are attached to the bottom wall and the air vortex moved upward to separate

the inlet flow stream from the exit air. For a fully open cavity, the flow seems to be complex and intensified relative to the partially opened cavity.
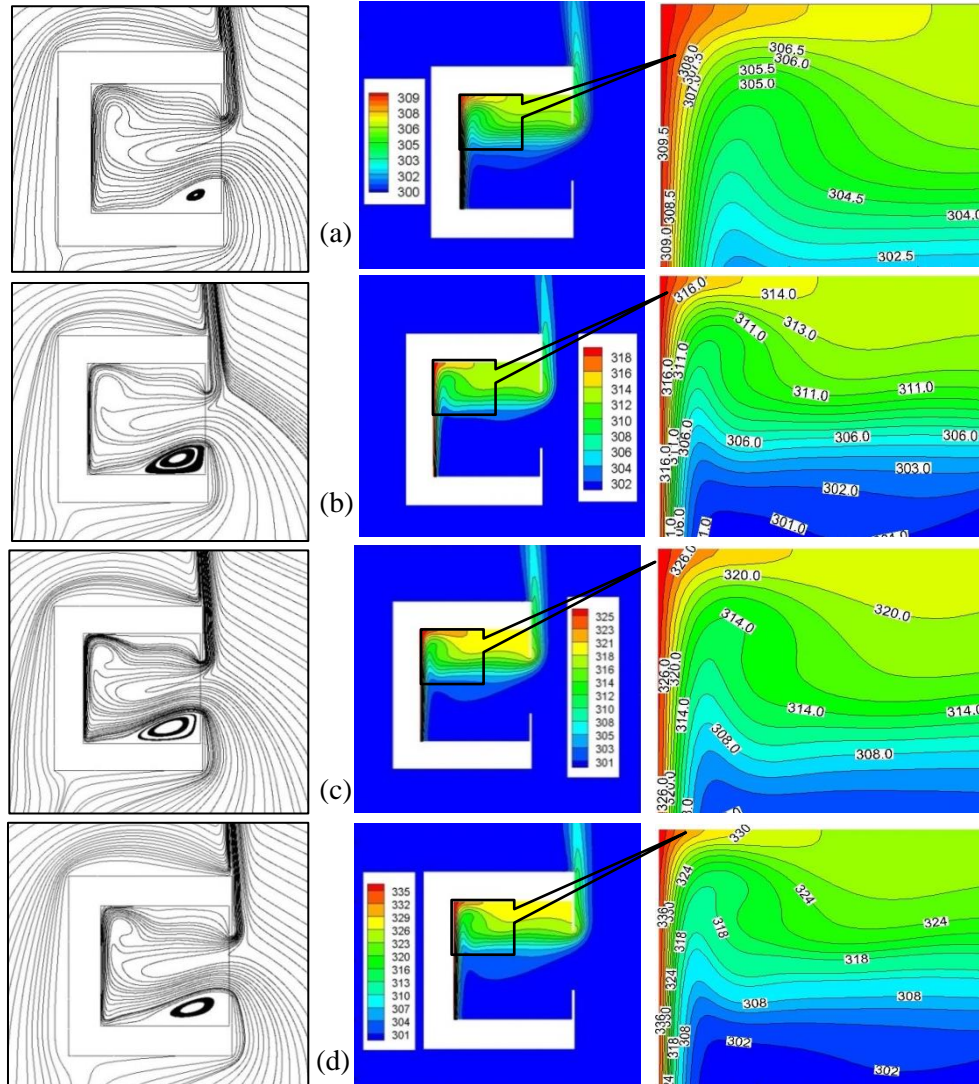

Figure 5: Stream function (on the left) and temperature (on the right) fields for the case $a/H = 0.50$, $\varphi = 0^0$: (a) $Ra = 9.41 \times 10^5$, (b) $Ra = 1.88 \times 10^6$, (c) $Ra = 2.826 \times 10^6$, (d) $Ra = 3.76 \times 10^6$
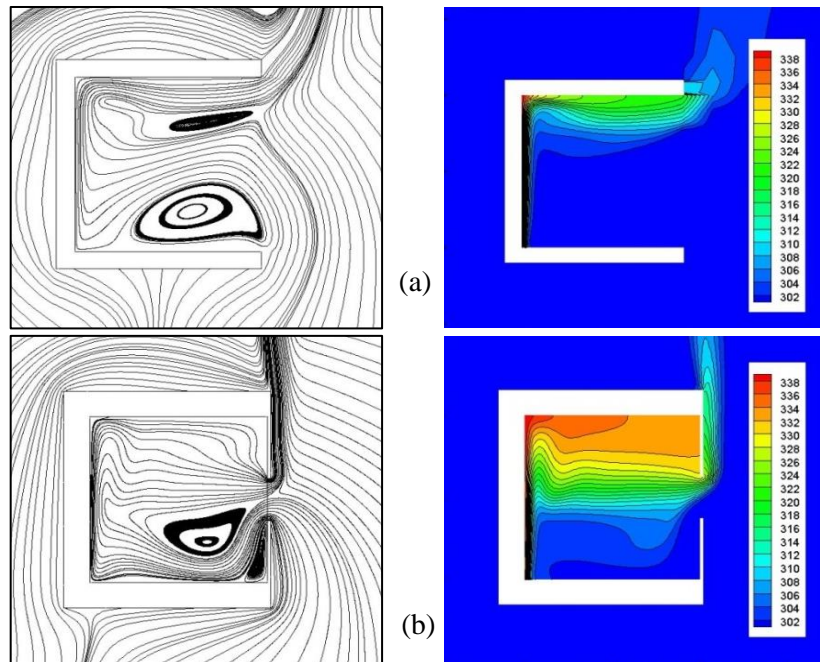
Figure 6: Stream function (on the left) and temperature (on the right) fields for the case,$\varphi = 0^0$,$Ra = 3.76 \times 10^6$ (a)$a/H = 1$, (b)$a/H = 0.25$

Fig. 7 presents the effect of inclination for the case of a/H=0.5, Ra=3.76×10^6 with φ from 15° to 90°. The case for φ=0° is shown in Fig. 5(d). We can observe that the upper part of the cavity experiences a trapped air vortex for the higher tilt angle, this is because the increase in the inclination and decrease in opening ratio cause higher wall shear flow and limited exit area. As a consequence the convective heat loss decreases.

The figure also shows that there is an increase in the thickness of the thermal boundary layer next to the hot wall and the boundary separating this area from the remaining part of the cavity becomes almost horizontal which can be considered as a stagnation boundary.

The region of the cavity above this plane is called "stagnation zone" while the below area is called "convective zone" where strong convective air currents are observed. This observation is confirmed in the literature. As the more increase in the cavity tilting up to 90° the more hot are trapped inside causing limited air to escape from the cavity and therefore limited air also to entry the cavity. The overall effect is low heat loss and reduction in convective heat strength.
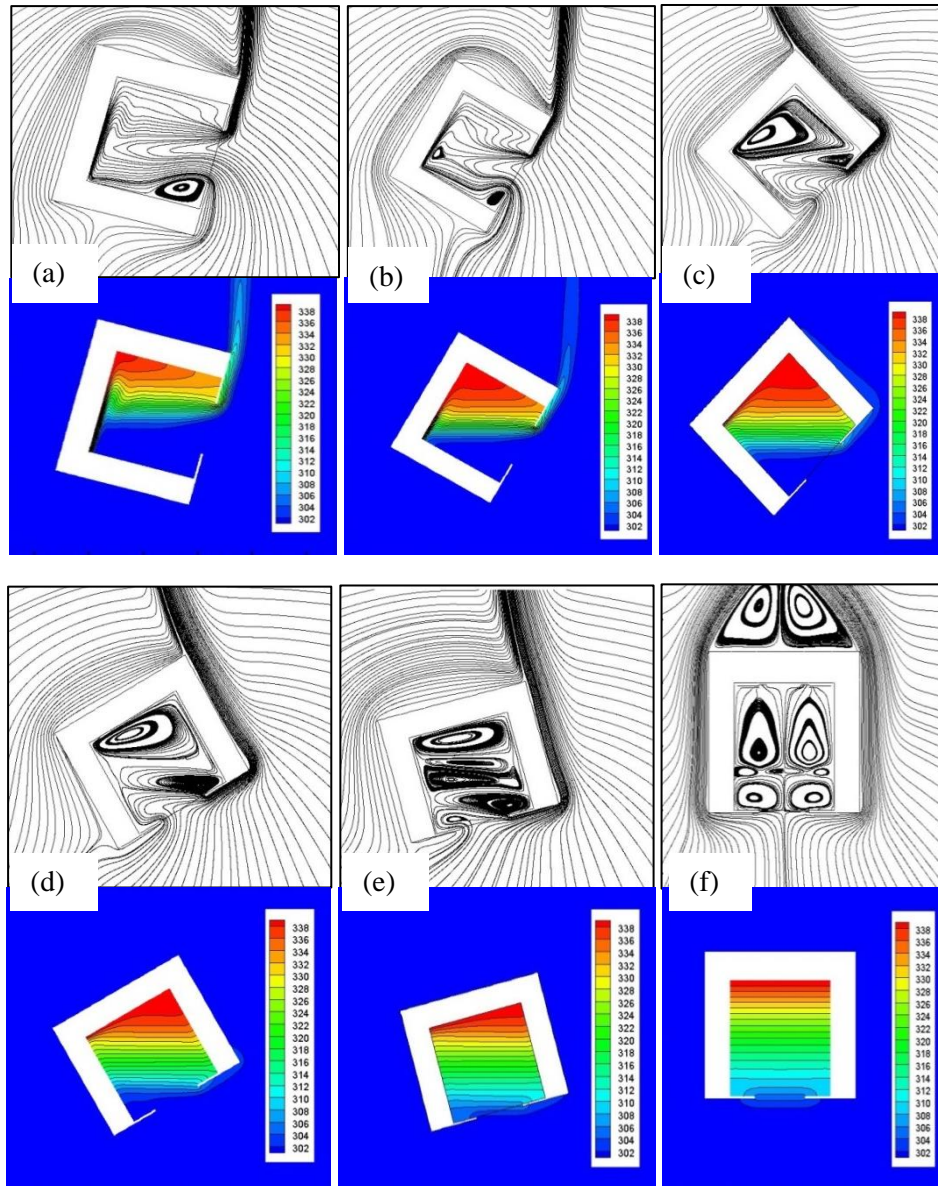
FDMP, vol.14, no.4, pp.223-242, 2018

Figure 7: Stream function (above) and temperature (below) fields for the case: a/H = 0.50, Ra = 3.76×10^6. (a) $\varphi = 15^0$, (b) $\varphi = 30^0$, (c) $\varphi = 45^0$, (d) $\varphi = 60^0$, (e) $\varphi = 75^0$, (f) $\varphi = 90^0$

5.2 Velocity and temperature profiles

In this section the velocity and temperature plots at the exit plane for three most important angles: 0°, 30° and 60° with an opening ratio of a/H = 0.5 are preseted Figs. 8 and 9. As shown in Fig. 8 the increase in the inclination angle from 0 to 60° strengthens

the air and mass entering and exiting the cavity. The effect of Rayleigh number on flow velocity and mass flow rate seem to be small, however it has an influence on the velocity distribution at the inlet and exit causing a shift of the peak velocity away from the cavity walls. It is also noticeable that as inclination angle decreased to 0°, the flow admitted to the cavity enhanced.
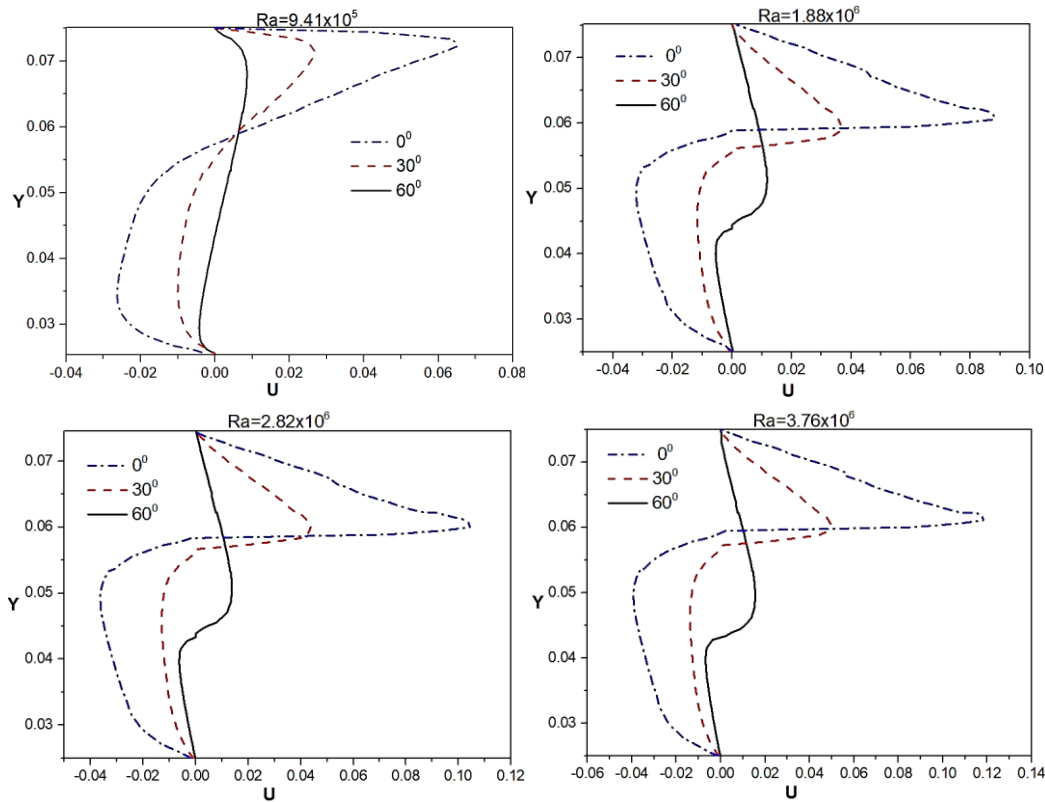

Figure 8: Velocity plots at exit plane for various tilt angles at fixed Rayleigh numbers and a/H = 0.5

In Fig. 9, for low angles 0° and 30°, the air enters at ambient temperature ($\theta = 0$, $T_\infty = 300$) then it is preheated before it reaches the back hot wall boundary layer. When the inclination angle is increased to 60° the temperature of the incoming air is slightly increased due to the stagnation. However, as Rayleigh number increases as the preheating of the incoming air decreases. Concerning the exiting flow, It is also observed that the exiting air temperature decrease with increasing the inclination angle, but increase when the Rayleigh number is increased.
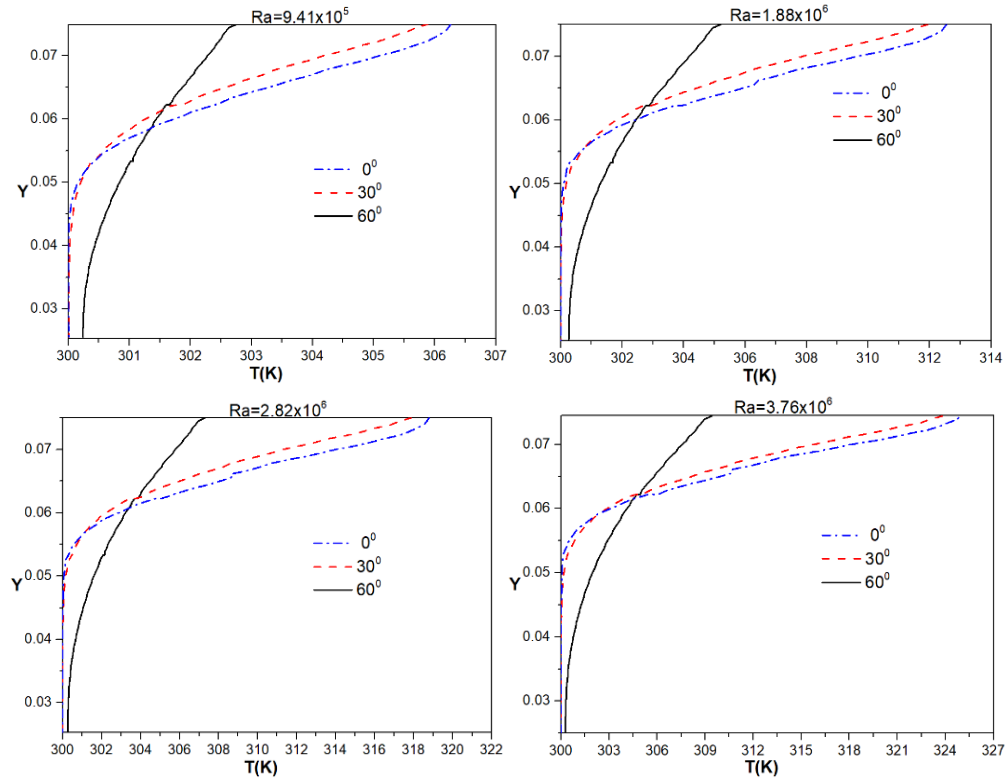
Figure 9: Temperature plots at exit plane for various tilt angles at fixed Rayleigh numbers and $a/H = 0.5$

5.3 Average Convective Nusselt number and heat loss

Figs. 10, 11 shows the average Nusselt number and convective heat loss Q_c values at the vertical hot wall for all the cases studied**.** The Nusselt number shows a non-linear variation with increasing inclination for all cases studied. Its maximum value reaches 20.47 at $\varphi=0°$, and $a/H=1$ and starts to decrease with increasing the angle to reach a minimum value 0.99 at $\varphi=90°$ and $a/H=1$. As inclination becomes high as Nusselt number is decreasing, except for $\varphi=60°$ to 90° with $a/H=0.25$ and 0.5 the average Nusselt number remains almost unchangeable. For the case: $a/H=1$, Nusselt number is constant with $\varphi=75°$ to 90°. The same behavior is observed concerning the convective heat loss Q_c except for angles: 60°, 75° and 90° ($a/H=0.25$, 0.5), and for $\varphi=75°$ to 90° ($a/H=1$) Q_c remain almost unchangeable.

While changing the tilt angle from 0° to 90°, the average Nusselt number is decreased by 93.49% for a fixed Rayleigh number, $Ra=3.76×10^6$ and opening ratio, $a/H=0.25$. Moreover, while changing the opening ratio from 1 to 0.25, the convective heat loss is reduced by 22.79% for a fixed Rayleigh number and tilt angle ($Ra=3.76×10^6$, $\varphi=0°$).
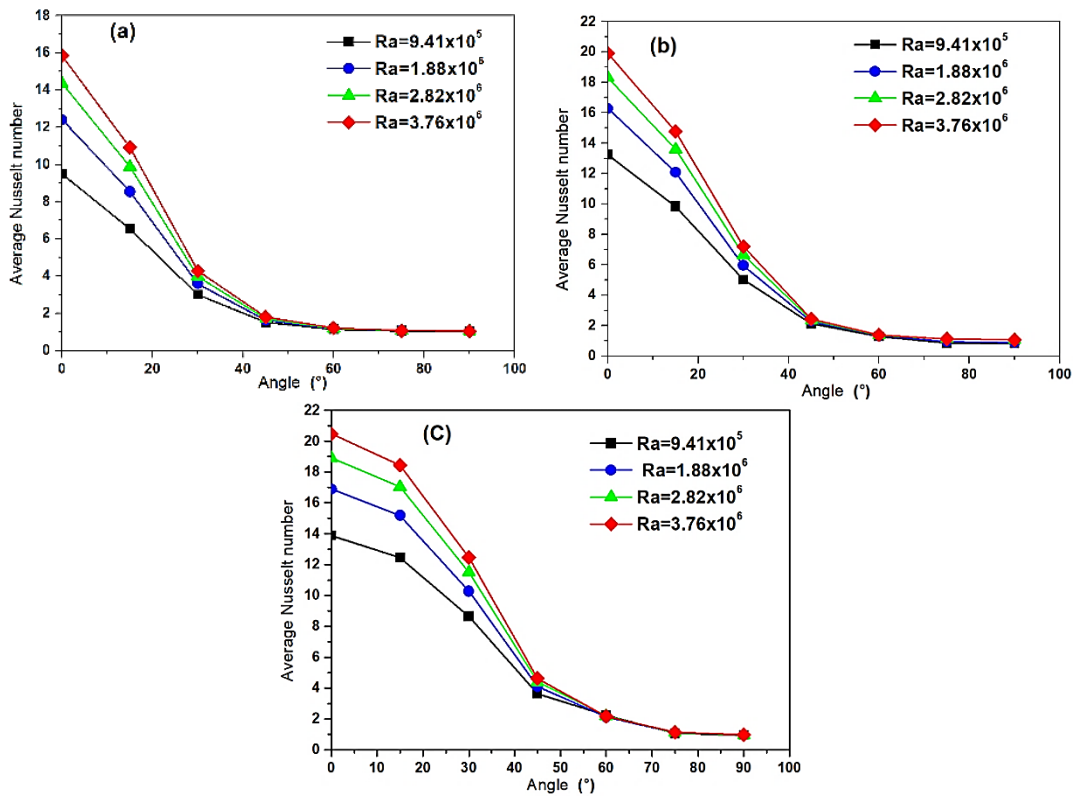
.

Figure 10: Average Nusselt number on the vertical hot wall for different inclination angle with opening ratios: (a) a/H=0.25, (b) a/H=0.5, (c) a/H=1

As a summary of the present calculations, correlations for the average Nusselt number was obtained using a least-square regression technique (computed data) and are given as:

For: $^a/_H = 0.25$, $Nu_c = 2.968 \times Ra^{0.333} \times \varphi^{-1.385}$ $(15^0 < \varphi < 90^0)$ (41)

For: $^a/_H = 0.5$, $Nu_c = 0.111 \times Ra^{0.232} \times \varphi^{-0.275}$ $(30^0 < \varphi < 90^0)$ (42)

For: $^a/_H = 1$, $Nu_c = 0.294 \times Ra^{0.28}$ $(\varphi = 0)$ (43)

The Nusselt correlation equation obtained using the results reported by Mohamad [Mohamad (1995)] and Hinojosa et al. [Hinojosa, Cabanillas and Alvarez (2005)] (for a/H = 1 , $\varphi = 0^0$) Where: $Nu_c = 0.22 \times Ra^{0.30}$ and, $Nu_c = 0.25 \times Ra^{0.29}$, Respectively. It can be seen that those equations are in good agreement with Eq. (43) obtained in this work.
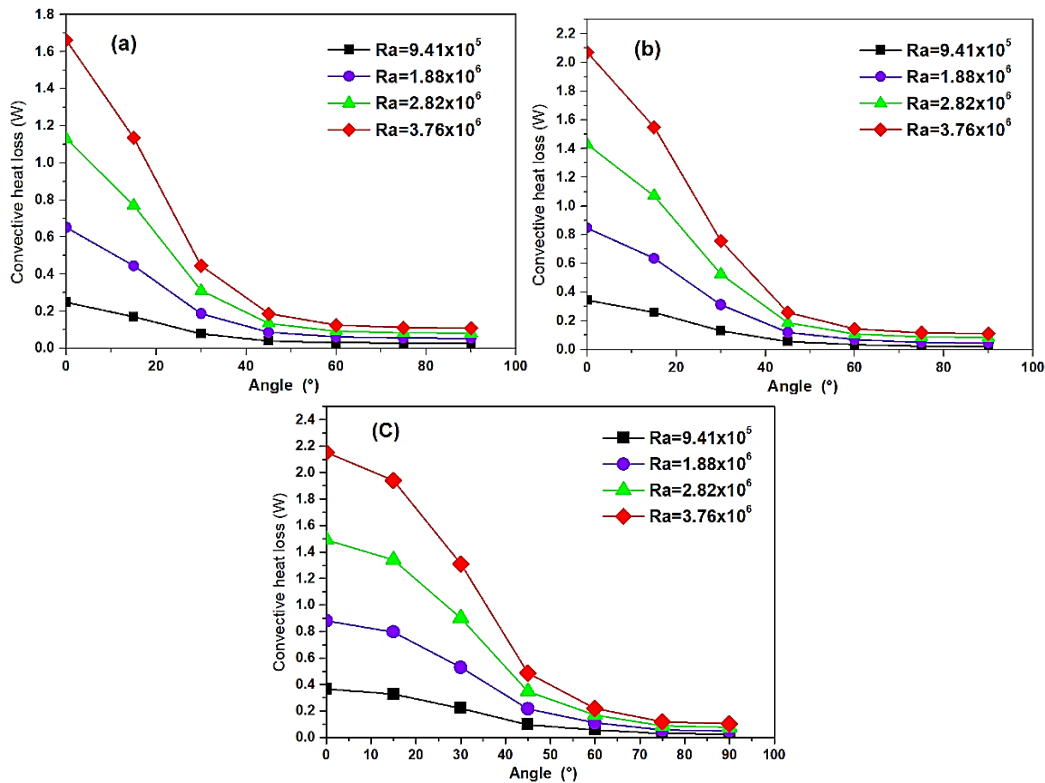
Figure 11: Convective heat loss at the vertical hot wall for different inclination angle with opening ratios: (a)a/H=0.25, (b)a/H=0.5, (c)a/H=1

6 Conclusions

In this work the numerical calculations of heat transfer by laminar natural convection in an inclined square solar cavity with three opening ratio are presented. The effect of geometrical and thermal parameters on the heat transfer are studied, and based on the numerical results a correlation of Nusselt number is proposed. It is valid for the opening ratios studied here and Ryaleight number 9.41×10^5 to 3.76×10^6. The correlation can be used to determine the convective heat losses from any square tilted solar cavity of opening ratio 0.25, 0.5 and 1 for industrial process heat or thermal power applications. The main observations can summarized as below:

- Increasing in the inclination and decreasing in the opening ratio result in the increase in the recirculation zone area within the cavity and therefore limiting convective zone, and accordingly, there is an increase in the thickness of the thermal boundary layer next to the vertical hot wall.

- The average Nusselt number decreases with increasing inclination angle for a fixed Rayleigh number and increase with the increasing Rayleigh number for a fixed angle; this can be explained by the behavior of the thermal boundary layer previously mentioned. For an angle of 60°, the average convective losses stay almost constant at (a/H=0.25, 0.5), and for φ=75° to 90° (a/H=1).

- For solar receiver applications, the smaller opening ratio for all angles studied is found to help in minimizing convective losses for solar cavities.

- The open cavity is found to exhibit its own strong flow characteristics near the opening and will be an interesting subject for further investigation.

- The flow throughout the open cavity depends strongly on the opening ratio, inclination angles and Rayleigh number.

The effect of radiation, wind condition, on the convective heat loss and Nusselt number, and determination of the performance of cavity receiver must be performed in future work, it can help in designing and optimizing the cavity heat receiver for both concentrating Solar Tower and Solar Parabolic Dish.

References

Adnani, M.; Meziani, B.; Ourrad, O.; Zitoune, M. (2016): Natural convection in a square cavity: Numerical study for different values of prandtl number. *Fluid Dynamics & Materials Processing*, vol. 12, no. 1, pp. 1-14.

Angirasa, D.; Eggels, J. G; Nieuwstadt, F. T. (1995): Numerical simulation of transient natural convection from an isothermal cavity open on a side. *Numerical Heat Transfer*, vol. 28, pp. 755-768.

Angirasa, D.; Pourquié, M. J.; Nieuwstadt, F. T. (1992): Numerical study of transient and steady laminar buoyancy-driven flows and heat transfer in a square open cavity. *Numerical Heat Transfer*, vol. 22, pp. 223-239.

Bensouici, F. Z.; Boudebous S. (2017): Mixed convection of nanofluids inside a lid-driven cavity heated by a central square heat source. *Fluid Dynamics & Materials Processing*, vol. 13, no. 3, pp. 189-212.

Chakroun, W.; Elsayed, M. M.; Al-Fahed, S. F. (1997): Experimental measurements of heat transfer coefficient in a partially/fully opened tilted cavity. *Journal of Solar Energy Engineering*, vol. 119, pp. 298-302.

Chan, Y. L.; Tien, C. L. (1985): A numerical study of two-dimensional laminar natural convection in shallow open cavities. *International Journal of Heat and Mass Transfer*, vol. 28, no. 3, pp. 603-612.

Clausing, A. M. (1981): An analysis of convective losses from cavity solar central receivers. *Solar Energy*, vol. 27, pp. 295-300.

Elsayed, M. M.; Al-Najem, N. M.; El-Refaee, M. M.; Noor, A. A. (1999): Numerical study of natural convection in fully open tilted cavities. *Heat Transfer Engineering*, vol. 20, no. 3, pp. 73-85.

Eymard, R.; Gallou, T.; Herbin, R. (2000): Finite volume methods. *Handbook of Numerical Analysis*, vol. 7, pp. 713-1020.

Hinojosa, J. F.; Cabanillas, R. E.; Alvarez, G.; Estrada, C. E. (2005): Nusselt Number for the natural convection and surface thermal radiation in a square tilted open cavity. *International Communications in Heat and Mass Transfer*, vol. 32, pp. 1184-1192.

Humphrey, J. A. C.; Sherman, F. S. (1985): Experimental study of free and mixed convective flow of air in a heated cavity. *Technical Report*. California University, Berkeley (USA).

Ka Lok, L.; Jafarian, M.; Farzin, G.; Maziar, A.; Graham, J. N. (2017): An investigation into the effect of aspect ratio on the heat loss from a solar cavity receiver. *Solar Energy*, vol. 149, pp. 20-31

Le Quere, P.; Humphrey, J. A. C.; Sherman, F. S. (1981): Numerical calculation of thermally driven two-dimensional unsteady laminar flow in cavities of rectangular cross section. *Numerical Heat Transfer*, vol. 4, pp. 249-283.

Manoj, T. K. R.; Rajsekhar, P. (2018): Numerical study of natural convection in a right triangular enclosure with sinusoidal hot wall and different configurations of cold walls. *Fluid Dynamics & Materials Processing*, vol. 14, no. 1, pp. 1-21.

Miyamoto, M.; Kuehn, T. H.; Goldstein, R. J. ; Katoh, Y. (1989): Two-dimensional laminar natural convection heat transfer from a fully or partially open square cavity. *Numerical Heat Transfer*, vol. 15, pp. 411-430.

Mohamad, A. (1995): Natural convection in open cavities and slots. *Numerical Heat Transfer*, vol. 27, pp. 705-716.

Nouri, S.; Ghezal, A.; Abboudi, S.; Spiteri, P. (2018): A numerical study of the transitions of laminar natural flows in a square cavity. *Fluid Dynamics & Materials Processing*, vol. 14, no. 2, pp. 121-135.

Patankar, S. V. (1980): *Numerical Heat Transfer and Fluid Flow*. McGraw-Hill Book Company, New York.

Penot, F. (1982): Numerical calculation of two-dimensional natural convection in isothermal open cavities. *Numerical Heat Transfer*, vol. 5, pp. 421-437.

Versteeg, H.; Malalasekera, W. (1995): An introduction to computational fluid dynamics. *The Finite Volume Method*, Longman Group Ltd.

Zhang, H. L.; Baeyens, J.; Degreve, J.; Caceres, G. (2013): Concentrated solar power plants: Review and design methodology. *Renewable and Sustainable Energy Reviews*, vol. 22, pp. 466-481.

Wang, Z.; Yang, M.; Li, L.; Zhang, Y. (2011): Combined heat transfer by natural convection-conduction and surface radiation in an open cavity under constant heat flux heating. *Numerical Heat Transfer*, vol. 60, pp. 289-304.